University of Nebraska - Lincoln

DigitalCommons@University of Nebraska - Lincoln

Evgeny Tsymbal Publications

Research Papers in Physics and Astronomy

12-10-2012

Ferroelectric Instability Under Screened Coulomb Interactions

Yong Wang
University of Nebraska - Lincoln

Xiaohui Liu
University of Nebraska-Lincoln, phyliuxiaohui@gmail.com

John D. Burton
University of Nebraska-Lincoln, jburton2@unl.edu

Sitaram S. Jaswal
University of Nebraska-Lincoln, sjaswal1@unl.edu

Evgeny Y. Tsymbal
University of Nebraska-Lincoln, tsymbal@unl.edu

Follow this and additional works at: http://digitalcommons.unl.edu/physicstsymbal

Part of the Condensed Matter Physics Commons

Ferroelectric Instability Under Screened Coulomb Interactions

Yong Wang,* Xiaohui Liu, J. D. Burton, Sitaram S. Jaswal, and Evgeny Y. Tsymbal†

*Department of Physics and Astronomy & Nebraska Center for Materials and Nanoscience, University of Nebraska,
Lincoln, Nebraska 68588, USA*

We explore the effect of charge carrier doping on ferroelectricity using density functional calculations and phenomenological modeling. By considering a prototypical ferroelectric material, $BaTiO_3$, we demonstrate that ferroelectric displacements are sustained up to the critical concentration of 0.11 electron per unit cell volume. This result is consistent with experimental observations and reveals that the ferroelectric phase and conductivity can coexist. Our investigations show that the ferroelectric instability requires only a short-range portion of the Coulomb force with an interaction range of the order of the lattice constant. These results provide a new insight into the origin of ferroelectricity in displacive ferroelectrics and open opportunities for using doped ferroelectrics in novel electronic devices.

Ferroelectric materials are characterized by the spontaneous electric polarization that can be switched between two (or more) orientations [1]. This property makes them attractive for technological applications, such as nonvolatile random access memories, ferroelectric field-effect transistors, and ferroelectric tunnel junctions [2–4]. The importance of ferroelectrics also stems from a fundamental interest in the understanding of the electric-dipole ordering, structural phase transitions, and symmetry breaking [5].

The perovskite ABO_3 ferroelectric compounds are an especially important group due to the relative simplicity of their atomic structure. The ferroelectric phase transition in these materials is a displacive transition from a high-symmetry paraelectric phase to a polar ferroelectric phase below the critical temperature [1]. This transition is characterized by a decreasing frequency of a transverse optical phonon mode (the soft mode) which drops to zero at the transition point and then becomes imaginary in the ferroelectric phase, corresponding to a collective displacement of ions from their centrosymmetric positions with no restoring force [6].

The ferroelectric instability can be explained by the interplay between long-range Coulomb interactions favoring the ferroelectric phase and short-range forces supporting the undistorted paraelectric structure [7]. Additional hybridizations between O cation $2p$ and metal anion d orbitals are required to diminish the short-range repulsion and thus to allow for the ferroelectric transition [8,9]. This view is supported by first-principles calculations which indicate that the large destabilizing Coulomb interaction yielding the instability is linked to giant anomalous Born effective charges arising due to the strong sensitivity of O–metal hybridizations to atomic displacements [10].

While doping a ferroelectric material may enhance its range of functionalities, charge carriers produced by doping screen the Coulomb interactions that favor the off-center displacements and eventually quench ferroelectricity.

This is why it is naturally expected that a ferroelectric phase could not exist in conducting materials. Contrary to this expectation, however, ferroelectric semiconductors have been known for a long time [11,12]. More recently ferroelectric displacements were observed in oxygen reduced conducting $BaTiO_{3-\delta}$ [13,14]. It was found that the ferroelectric instability is sustained up to a critical electron concentration $n \approx 1.9 \times 10^{21}$ cm^{-3}, which corresponds to about 0.1 e per unit cell (u.c.) of $BaTiO_3$.

The origin of this "metallic ferroelectricity" is directly related to several important and interesting fundamental questions [15]. How does the screening of the Coulomb interaction affect the ferroelectric displacements? What is the minimum effective range of the Coulomb force to preserve the ferroelectric instability? What happens with the soft mode with charge doping? The answers to these questions would not only provide a better understanding of the nature of ferroelectricity, but also open new possibilities for functional materials.

In this Letter, we explore the charge carrier doping effect on ferroelectricity using density functional calculations along with phenomenological modeling based on screened long-range Coulomb interactions and the short-range bonding and repulsion effects. By considering a prototypical ferroelectric material, $BaTiO_3$, we demonstrate that ferroelectric displacements are sustained in the electron doped material up to a critical concentration of 0.11 electron per unit cell volume, thus revealing that the ferroelectric phase and conductivity can coexist. Our investigations show that the ferroelectric instability requires only a short-range portion of the Coulomb force with an interaction range of the order of the lattice constant.

We employ density functional theory (DFT) implemented in the plane-wave pseudopotential code QUANTUM-ESPRESSO [16]. The exchange and correlation effects are treated within the local-density approximation. The electron wave functions are expanded in a plane-wave basis set

limited by a cutoff energy of 600 eV. $14 \times 14 \times 14$ and $24 \times 24 \times 24$ Monkhorst-Pack k point meshes are used for structural relaxation and density of states (DOS) calculations, respectively. The self-consistent calculations are converged to 10^{-5} eV/u.c. The atomic positions are obtained by fully relaxing the lattice and all the ions in the unit cell until the Hellmann-Feynman force on each atom becomes less than 5 meV/Å. The electron doping in BaTiO$_3$ is achieved by adding extra electrons to the system with the same amount of uniform positive charge in the background. For the undoped tetragonal BaTiO$_3$, our calculation gives the lattice constant $a = 3.933$ Å and $c/a = 1.015$, polarization $P = 28.6$ μC/cm^2, and Ti-O and Ba-O relative displacements of 0.113 and 0.091 Å, respectively, consistent with previous local-density approximation calculations [5]. We note that effects of carrier doping on polarization of BaTiO$_3$, which includes both the ionic and electronic contributions, cannot be calculated using the Berry phase method [17]. Therefore, in this Letter we focus on analyzing the ionic ferroelectric-like displacements and the phonon frequency of the soft mode.

Doping BaTiO$_3$ with electrons pushes the Fermi energy, E_F, into the conduction band and screens the electric potential of an ionic charge. Figure 1 shows the DOS of BaTiO$_3$ for different electron doping concentrations n. A typical scale associated with screening is the screening length, λ, which depends on n. We estimate the screening length using the Thomas-Fermi model according to which $\lambda = \sqrt{\varepsilon / e^2 D(E_F)}$. Here, $D(E_F)$ is the DOS at E_F and ε is the dielectric permittivity of undoped BaTiO$_3$ at saturation polarization, which we assume to be $\varepsilon \approx 44\varepsilon_0$ [18]. Undoped BaTiO$_3$ ($n = 0$) is an insulator so that $D(E_F) = 0$ and hence λ is infinite. As n becomes larger, more conduction band states are populated (Fig. 1), thus increasing $D(E_F)$ and reducing the screening length. As
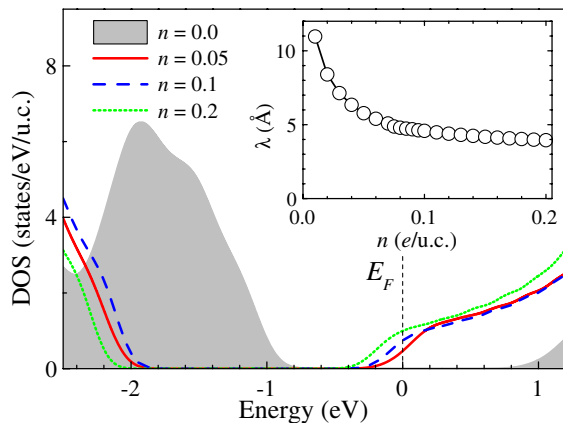
seen from the inset in Fig. 1, when n is raised up to 0.2 e/u.c. λ decreases down to about 4 Å.

Next, we study the effect of screening due to electron doping on the ferroelectric displacements in BaTiO$_3$. Figure 2(a) shows the calculated displacements between M and O ($M =$ Ti, Ba) ions as a function of n. Surprisingly, we find that ferroelectric displacements hardly change with electron doping up to n as high as 0.05 e/u.c, and then decay very fast and vanish above the critical electron concentration $n_c = 0.11$ e/u.c. The c/a ratio of BaTiO$_3$ under the increasing n, as shown in Fig. 2(b), also displays a similar critical behavior as that of polar displacements. BaTiO$_3$ transforms from the tetragonal phase with $c/a = 1.015$ to the cubic phase with $c/a = 1.0$ at $n_c = 0.11$ e/u.c. The critical doping concentration n_c found from first-principles is consistent with the experimental result [13]. According to the inset in Fig. 1, the critical electron concentration $n_c = 0.11$ e/u.c. corresponds to a screening length $\lambda_c \approx 5$ Å. Therefore, we conclude that only the short-range Coulomb forces with the interaction range comparable to the lattice constant are responsible for maintaining ferroelectric instability in BaTiO$_3$.

Since changes in hybridization with doping can also affect ferroelectric displacements, we calculate the occupation numbers N_d for the Ti-3d orbitals ($3d_{z^2}$, $3d_{x^2-y^2}$, $3d_{xy}$, $3d_{xz,yz}$) and N_p for the O-2p orbitals of BaTiO$_3$ for different n. These occupations reflect the degree of hybridization between Ti-3d and O-2p orbitals. As seen in Fig. 3, N_d decreases and N_p increases very slowly with increasing n, so that their change is very small when n is altered from 0 to $n_c = 0.11$ e/u.c. This suggests that the changes in hybridization with doping are negligible. Thus, the dominant mechanism contributing to the ferroelectric critical behavior in n-doped BaTiO$_3$ is the screening of Coulomb interactions.
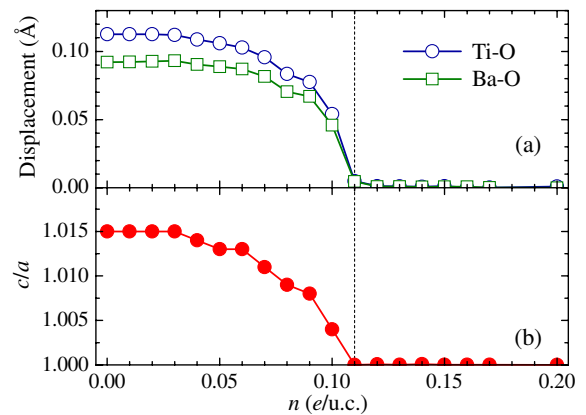

FIG. 1 (color online). DOS of BaTiO$_3$ for different electron doping concentrations n given in units of e/u.c. The shaded plot is the DOS of undoped BaTiO$_3$. The vertical dashed line denotes the Fermi energy. The inset shows the Thomas-Fermi screening length λ as a function of n.

FIG. 2 (color online). M-O ($M =$ Ti, Ba) relative displacements in BaTiO$_3$ (a) and the ratio of out-of-plane lattice constant c and in-plane lattice constant a (b) as a function of electron doping concentration n. The dashed line indicates the critical value n_c.
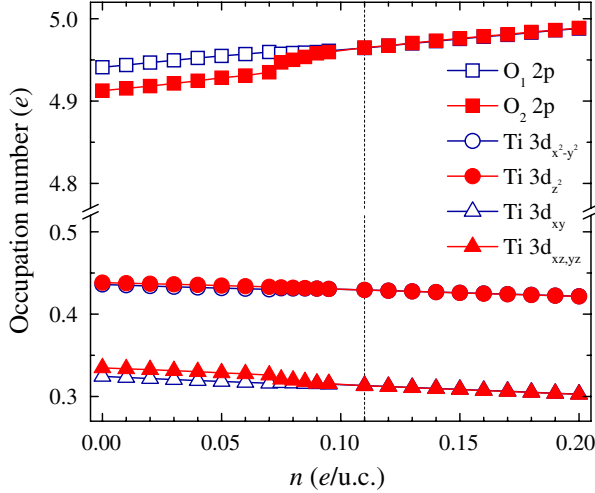
FIG. 3 (color online).   Occupation numbers for Ti-3d and O-2p orbitals as a function of electron concentration n. O$_1$ (O$_2$) correspond to O atoms lying in (off) the TiO$_2$ plane.

FIG. 4 (color online). M-O (M = Ti, Ba) relative displacements and phonon frequency of the soft mode at the Γ point in cubic BaTiO$_3$ as a function of electron concentration. The negative sign of the frequency indicates an imaginary value of the frequency.

This assertion is further confirmed through our calculations of p-doped BaTiO$_3$. Adding holes in BaTiO$_3$ places the Fermi energy in the valence band that is largely determined by the O-2p orbitals. This is different from the n-doped BaTiO$_3$, where the E_F lies in the conduction band built up of the Ti-3d bands. Despite this difference in the bands involved, we find that the p-doped BaTiO$_3$ demonstrates a similar critical behavior of ferroelectric displacements with a critical hole concentration $p_c \approx 0.12e$/u.c. We note that previous theoretical studies of the hole doping of BiFeO$_3$ predicted a possibility of enhanced ionic off-centering in this material [19]. We did not find such a trend in our calculations of p-doped BaTiO$_3$.

The signature of the ferroelectric phase transition can also be seen from the softening of the phonon mode in the paraelectric phase when approaching the critical point with the frequency becoming imaginary in the ferroelectric phase [6]. To confirm the phase transition at the critical concentration we have performed phonon calculations within the density functional perturbation theory, as implemented in QUANTUM-ESPRESSO. In these calculations we consider cubic BaTiO$_3$ with the lattice constant fully relaxed. Figure 4 shows the lowest frequency of the triple degenerate phonon mode at the Γ point as a function of electron concentration n, along with the relative cation-anion displacements. We see that the frequency remains imaginary up to an electron concentration as high as 0.11 e/u.c. and becomes real above this critical concentration. This critical behavior of the ferroelectric instability is echoed by the cation-anion displacements in cubic BaTiO$_3$ shown in this figure.

To further understand the critical behavior of ferroelectricity due to screened Coulomb interactions, we have developed a physically realistic model explicitly including the scre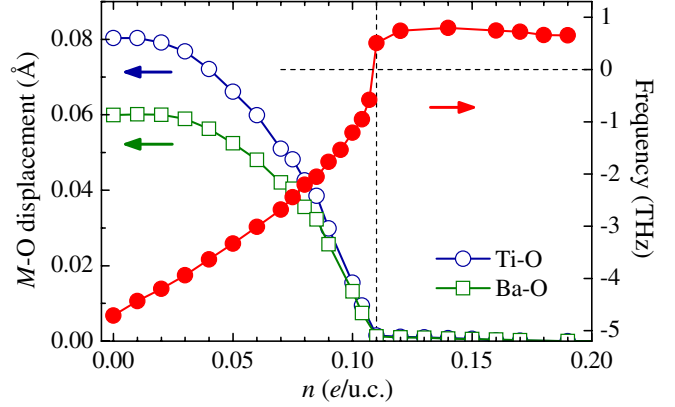ening effect. We consider a three-dimensional lattice of ions in the cubic perovskite structure. In the Thomas-Fermi approximation each ion is shrouded by an exponentially decaying screening charge density with screening length λ. The analytical form of the Coulomb interaction energy w_{ij} between two screened point charge q_i and q_j at locations $\mathbf{r}_i$ and $\mathbf{r}_j$, respectively, is $w_{ij}(|\mathbf{r}_i - \mathbf{r}_j|) = q_i q_j w(d)$, where

$$w(d) = \frac{1}{4\pi\varepsilon_0 d}\left(1 - \frac{d}{2\lambda}\right)e^{-d/\lambda} \qquad (1)$$

and $d = |\mathbf{r}_i - \mathbf{r}_j|$ is the distance between the two ions (see Supplemental Material [20]). The factor $(1 - d/2\lambda)e^{-d/\lambda}$ in Eq. (1) is the distance and screening length dependent coefficient, which reflects the effect of screening and converges to 1 as $\lambda \to \infty$. The electrostatic energy per unit cell is given by a lattice sum over all interaction terms of the form (1)

$$W = \frac{1}{2}\sum_{\mathbf{R}}\sum_{i,j=1}^{5}{}' q_i q_j w(|\mathbf{r}_i - \mathbf{r}_j + \mathbf{R}|), \qquad (2)$$

where $\mathbf{R} = a\,(m_x, m_y, m_z)$ are lattice vectors with the m running over all integers. The prime sign on the summation in Eq. (2) indicates that for the $\mathbf{R} = 0$ terms, $i = j$ should be excluded to avoid self-interactions and the factor of $1/2$ takes care of double counting. The summation in Eq. (2) is performed in the spirit of an Ewald sum (see Supplemental Material [20]).

In addition to the long-range electrostatic energy, short-range Ba-O, O-O and Ti-O interactions are also included in the model. These interactions are described by Lennard-Jones potentials $E_0[(R_0/r)^7 - 2(R_0/r)^6]$, along with a O-Ti-O three body potentials given by $k_2(\theta - \theta_0)^2/2$, as parameterized in Ref. [21]. The potential parameters are fitted to obtain the same Ba-O and Ti-O displacements in undoped BaTiO$_3$ as those found by our DFT calculations.
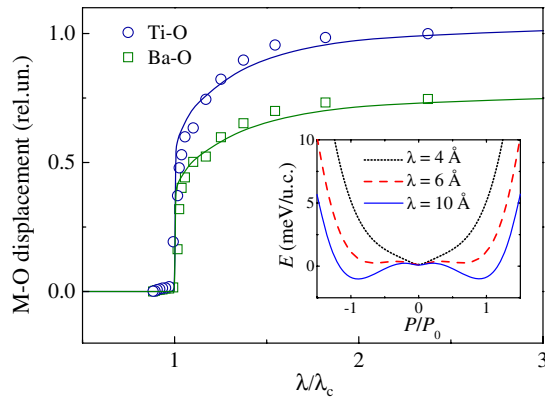
FIG. 5 (color online). M-O (M = Ti, Ba) relative displacements (in relative units) in cubic BaTiO$_3$ as predicted by the phenomenological model (solid lines) and DFT calculation (open symbols). The latter are the same as those in Fig. 4 but plotted versus λ/λ_c according to the Thomas-Fermi relationship between λ and n displayed in the inset of Fig. 1. The inset shows the total energy versus relative polarization for different values of λ, as follows from the phenomenological model.

All the parameters of the model except λ are now fixed throughout the calculation.

The total energy of undoped BaTiO$_3$ obtained by adding all the energies described above yields a typical potential [5] with minima at two nonzero polarizations, as seen from the inset in Fig. 5. As the electron screening length λ begins to decrease with increasing doping, these minima become shallower slowly in the beginning. When λ approaches the critical value of λ_c, the two wells flatten quite rapidly. For $\lambda < \lambda_c$, the wells merge into a single well at $P = 0$ indicating a first-order phase transition to the paraelectric phase. The critical value predicted by the model, $\lambda_c \approx 5.3$ Å, is consistent with that obtained from the Thomas-Fermi estimate based on the DFT calculations. Figure 5 shows M-O displacements versus the normalized screening length. It is seen that the critical behavior predicted by our model (solid lines) is in agreement with our DFT calculation (open symbols). Thus, our phenomenological model confirms the fact that only a short range portion of the Coulomb interaction is required to sustain ferroelectric displacements.

The coexistence of the ferroelectric phase and conductivity is interesting for device applications because such a conducting bistable material has new functionalities. Although in such a material an external electric field induces a flow of electric current which makes switching of the ferroelectric displacements difficult, sufficiently resistive materials may sustain the coercive voltage. For example, ferroelectric tunnel junctions are switchable despite the current flowing across them [22]. Furthermore, ferroelectric switching can be realized by the applied voltage which rises sufficiently fast in time. A recent prominent example is the resistive switching behavior of semiconducting ferroelectric BiFeO$_3$ [23]. Also, there exist means to switch ferroelectrics

with no applied voltage [24]. Doped ferroelectrics may have implications in magnetoelectric devices where the interface magnetization is affected by the ferroelectric polarization charge [25,26].

In conclusion, using first-principles calculations and a phenomenological model we have demonstrated that ferroelectric displacements are well preserved in doped BaTiO$_3$ until the doping concentration exceeds a critical value of $n_c = 0.11$ e/u.c. This critical behavior is due to the electron screening of the Coulomb interactions responsible for the ferroelectric instability. The critical screening length is found to be surprisingly small, about 5 Å, demonstrating that "short-range" Coulomb interactions are sufficient to lead to collective ferroelectric displacements. This value may be considered as a qualitative estimate for a lower limit for the critical size of BaTiO$_3$ of a few unit cells for the existence of ferroelectricity. Our results provide a new insight into the origin of ferroelectricity in displacive ferroelectrics and open opportunities for using doped ferroelectrics in novel electronic devices.

*Present address: Pacific Northwest National Laboratory, Richland, Washington 99352, USA.
†tsymbal@unl.edu

[1] M. E. Lines and A. M. Glass, *Principles and Applications of Ferroelectrics and Related Materials* (Clarendon Press, Oxford, 1977).

[2] M. Dawber, K. M. Rabe, and J. F. Scott, Rev. Mod. Phys. **77,** 1083 (2005).

[3] N. Setter, D. Damjanovic, L. Eng, G. Fox, S. Gevorgian, S. Hong, A. Kingon, H. Kohlstedt, N. Y. Park, G. B. Stephenson, I. Stolitchnov, A. K. Tagantsev, D. V. Taylor, T. Yamada, and S. Streiffer, J. Appl. Phys. **100,** 051606 (2006).

[4] E. Y. Tsymbal, A. Gruverman, V. Garcia, M. Bibes, and A. Barthélémy, MRS Bull. **37,** 138 (2012).

[5] *Physics of Ferroelectrics: A Modern Perspective*, edited by K. Rabe, C. H. Ahn, and J.-M. Triscone (Springer, New York, 2007).

[6] W. Zhong, R. D. King-Smith, and D. Vanderbilt, Phys. Rev. Lett. **72,** 3618 (1994).

[7] W. Cochran, Adv. Phys. **9,** 387 (1960).

[8] R. E. Cohen, Nature (London) **358,** 136 (1992).

[9] N. A. Hill, J. Phys. Chem. B **104,** 6694 (2000).

[10] P. Ghosez, J.-P. Michenaud, and X. Gonze, Phys. Rev. B **58,** 6224 (1998).

[11] J. F. Scott, Rev. Mod. Phys. **46,** 83 (1974).

[12] V. Fridkin, *Ferroelectric Semiconductors* (Consultants Bureau, New York, 1980), p. 318.

[13] T. Kolodiazhnyi, M. Tachibana, H. Kawaji, J. Hwang, and E. Takayama-Muromachi, Phys. Rev. Lett. **104**, 147602 (2010).

[14] J. Hwang, T. Kolodiazhnyi, J. Yang, and M. Couillard, Phys. Rev. B **82**, 214109 (2010).

[15] P. W. Anderson and E. I. Blount, Phys. Rev. Lett. **14**, 217 (1965).

[16] P. Giannozzi *et al.*, J. Phys. Condens. Matter **21**, 395502 (2009).

[17] R. Resta, Ferroelectrics **136**, 51 (1992); R. D. King-Smith and D. Vanderbilt, Phys. Rev. B **47**, 1651 (1993).

[18] G. Rupprecht and B. O. Bell, Phys. Rev. **135**, A748 (1964).

[19] D. Ricinschi and M. Okuyama, Ferroelectrics **355**, 101 (2007).

[20] See Supplemental Material at http://link.aps.org/supplemental/10.1103/PhysRevLett.109.247601 for details.

[21] C. L. Freeman, J. A. Dawson, H.-R. Chen, J. H. Harding, L.-B. Ben, and D. C. Sinclair, J. Mater. Chem. **21**, 4861 (2011).

[22] A. Gruverman, D. Wu, H. Lu, Y. Wang, H. W. Jang, C. M. Folkman, M. Y. Zhuravlev, D. Felker, M. Rzchowski, C.-B. Eom, and E. Y. Tsymbal, Nano Lett. **9**, 3539 (2009).

[23] A. Q. Jiang, C. Wang, K. J. Jin, X. B. Liu, J. F. Scott, C. S. Hwang, T. A. Tang, H. B. Lu, and G. Z. Yang, Adv. Mater. **23**, 1277 (2011).

[24] H. Lu, C.-W. Bark, D. E. de los Ojos, J. Alcala, C. B. Eom, G. Catalan, and A. Gruverman, Science **336**, 59 (2012).

[25] J. P. Velev, S. S. Jaswal, and E. Y. Tsymbal, Phil. Trans. R. Soc. A **369**, 3069 (2011).

[26] M. K. Niranjan, J. D. Burton, J. P. Velev, S. S. Jaswal, and E. Y. Tsymbal, Appl. Phys. Lett. **95**, 052501 (2009).